Catena 169 (2018) 128–139

Contents lists available at ScienceDirect

Catena

journal homepage: www.elsevier.com/locate/catena

Dynamic changes of soil erosion in a typical disturbance zone of China's Three Gorges Reservoir

Yuhai Bao[a,*], Xiubin He[a], Anbang Wen[a], Peng Gao[b,*], Qiang Tang[a,c], Dongchun Yan[a], Yi Long[a]

[a] Key Laboratory of Mountain Surface Processes and Ecological Regulation, Institute of Mountain Hazards and Environment, Chinese Academy of Sciences, Chengdu 610041, China

[b] Department of Geography, Syracuse University, Syracuse, NY 13244, USA

[c] Sustainable Agriculture Sciences Department, Rothamsted Research, North Wyke, Okehampton, Devon EX20 2SB, UK

ARTICLE INFO

Keywords:
Soil erosion
Temporal and spatial changes
Reservoir disturbance zone
Three Gorges Reservoir

ABSTRACT

The water level fluctuation region in China's Three Gorges Reservoir (TGR) represents a disturbance zone that experiences cyclic exposure and inundation due to reservoir operations. This area has also been subjected to long periods of flooding and wave-induced scouring. Thus, soil erosion in the disturbance zone has greatly intensified since the reservoir was first filled in 2006. In this study, soil erosion rates along nine transects in the mainstream disturbance zone (MDZ) and three transects in a tributary disturbance zone (TDZ) were continuously measured between 2008 and 2016 using erosion pins. The results showed that the average erosion rate in the MDZ was 32 mm yr^{-1}, which was more than six times greater than that in the TDZ. Spatially, the soil erosion rates in the MDZ displayed higher variability than those in the TDZ. The highest rate was found for the altitude range of 170–175 m in the MDZ, and the rates in the altitude ranges decreased in the order of 145–150 m, 160–165 m, and 165–170 m. However, the spatial variation of soil erosion rates in the TDZ was less significant than that in the MDZ. Furthermore, soil erosion rates in the MDZ displayed a small decreasing trend over the first six years and a much greater decreasing trend in the following three years. In contrast, these rates decreased significantly and continuously from 2008 to 2016 in the TDZ. The mean reduction rate of soil erosion in the MDZ was statistically higher than that in the TDZ. The annual average value of soil erosion rate reduction from all transects in the MDZ was 4.1 mm yr^{-1}, whereas it was only 1.7 mm yr^{-1} in the TDZ. Changes in hydrological regime, vegetation cover, and slope gradient were the main factors that governed the spatial and temporal patterns of soil erosion in the disturbance zone of the TGR.

1. Introduction

A reservoir disturbance zone (RDZ) generally refers to all landforms along river banks that fall between the peak and base water levels produced by regular dam operation (Bao et al., 2015a). RDZs have also been used to refer to shorelines, beaches, and banks in many studies as they denote similar types of water level fluctuation areas around reservoirs and lakes throughout the world (e.g., Cyberski, 1973; Buckler and Winters, 1983; Carter et al., 1986; Lawrence, 1994; Tommaselli et al., 2014; de Moraes et al., 2016; Sadeghian et al., 2017). RDZs typically have sharp biological and physical gradients along bank slopes. RDZs represent a hydrogeomorphological and biogeochemical ecotone between aquatic and terrestrial ecosystems and have been well recognized as a key area for maintaining ecosystem goods and services, including bank stabilization, biodiversity conservation, runoff regulation, pollutant interception, and amenity value (Naiman and Decamps, 1997; Lowrance et al., 2000; Anbumozhi et al., 2005; Mander et al., 2005; Kenwick et al., 2009; Cheng et al., 2010; Yang et al., 2012; Bao et al., 2015a).

However, RDZs are ecologically fragile due to issues caused by frequent water level fluctuations (New and Xie, 2008; Chang et al., 2011). One of these issues is related to the highly dynamic morphological changes resulting from soil erosion and sediment deposition. Soil erosion is an overall consequence of multiple complex processes, such as crumbling, scouring, scattering, and slumping (Cyberski, 1973; Born and Stephenson, 1973). Field monitoring and modeling have revealed that soil erosion in the RDZ is complex and highly variable (Pincus, 1962; Gatto and Doe, 1987; Carter and Guy, 1988; Hubertz et al., 1991; Saint-Laurent et al., 2001; Siqueira et al., 2015). Soil erosion rates may be extremely high during the initial period of reservoir impoundment when reservoir banks become unstable under changing fluvial hydrodynamics (Nilsson et al., 1997; Zhang, 2009; Vilmundardóttir et al.,

* Corresponding authors.
E-mail addresses: byh@imde.ac.cn (Y. Bao), pegao@maxwell.syr.edu (P. Gao).

https://doi.org/10.1016/j.catena.2018.05.032
Received 22 August 2017; Received in revised form 23 May 2018; Accepted 25 May 2018
Available online 01 June 2018

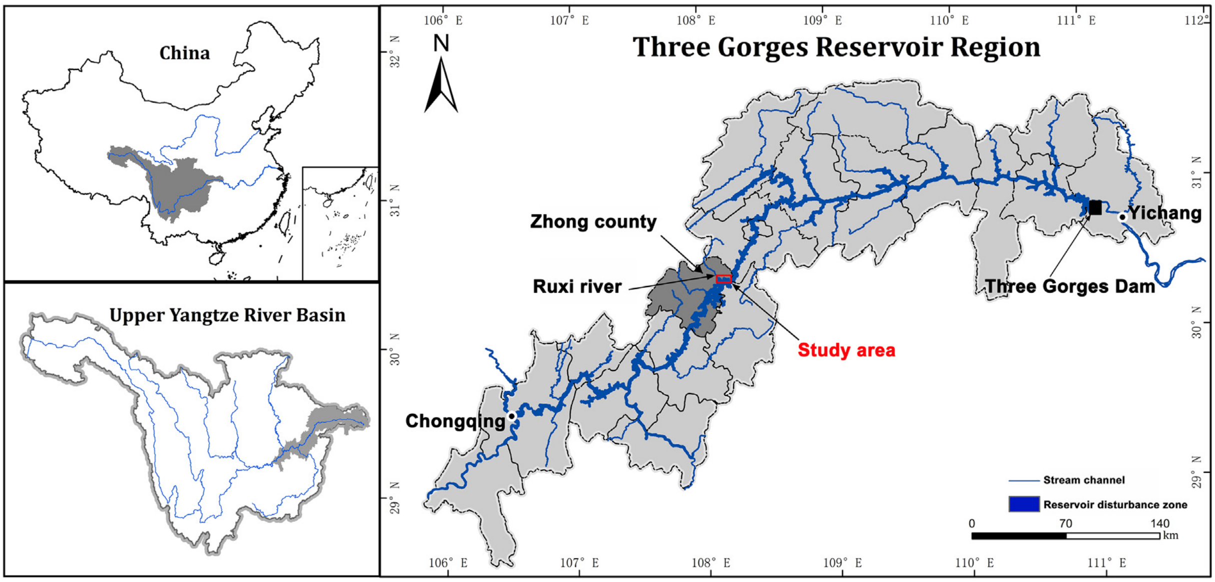

Fig. 1. Location of China's Three Gorges Reservoir and the study area.

2010; Kaczmarek et al., 2016). Soil erosion in the RDZ may cause a series of social and environmental consequences, including (i) reduced reservoir storage capacity caused by siltation (Hagan and Roberts, 1972; Seversona et al., 2009; Bao et al., 2010), (ii) generation of complex sources of water pollution (Tang et al., 2014a & 2014b), (iii) reduced habitats and biodiversity in the RDZ (New and Xie, 2008), and (iv) fragmented landscapes and disturbed ecosystem integrity. To date, > 50,000 reservoirs of various sizes have been constructed in the Yangtze River basin, with many other dams proposed for construction by 2020 (Li et al., 2013). Therefore, successful management of environmental problems related to reservoirs requires an understanding of the dynamic changes in soil erosion in the RDZ (Wu et al., 2004; New and Xie, 2008).

The Three Gorges Dam on the Upper Yangtze River is a typical valley dammed reservoir, which is part of the world's largest hydroelectric power plant and is categorized by an unprecedented RDZ. Understanding the change in soil erosion in response to disturbances caused by the changed hydrological regime in the disturbance zone (DZ) of the Three Gorges Reservoir (TGR) in China is particularly vital, given that most studies have been carried out in regions outside of China, such as the northern United States, Canada, Poland, and the former Soviet Union (e.g., Kondratjev, 1966; Cyberski, 1965 & 1973; Avakyn, 1975; Shur et al., 1978; Lukac, 1982; Reid, 1985; Lawson, 1985; Gatto and Doe, 1987; Reid et al., 1988; Sadeghian et al., 2017). Most studies of reservoir bank erosion have taken place in cold or temperate regions, with only a few studies in tropical regions (Fernandez and Fulfaro, 2000; Siqueira et al., 2015). The TGR is located across subtropical climate regions; it was completed in 2006 and has been in regular operation since 2010. Since the reservoir's impoundment, an RDZ has been created as a result of controlling the water flow. The RDZ is characterized by variations in the annual cyclic water level in conjunction with additional changes caused by rainfall events during the wet season. In particular, the magnitude and frequency of the flow in this zone are controlled by the 30 m change in water level over one annual cycle. Since 2010, multiple processes, including ecological degradation in terms of vegetation loss and habitat fragmentation and geomorphological adjustments through bank erosion and sedimentation, have been evident in the RDZ of the TGR (Bao et al., 2015b). Moreover, the morphology of the RDZ has constantly changed due to active erosion and deposition processes. However, the combined effect of these processes on the RDZ and the associated morphological responses remain to be studied, which has halted the progress of understanding the geochemical and biological processes that are linked to the increasing pollution and destruction of the ecosystem in the RDZ. The complex interactions among geomorphological, geochemical, and ecological processes have made the RDZ a unique geomorphological unit. Understanding the geomorphological processes will provide new insight into the effect of the RDZ on water quality and the ecological environment of the TGR (Bao et al., 2015a), which may help to improve the management of cascade reservoirs in China as well as those in countries around the world.

The DZ of the TGR is an artificial reservoir transitional zone that significantly affects the health of the reservoir. The morphological changes in the RDZ are subjected to fluvial processes driven by the annual cyclic variation of the water level, as well as storm events. Therefore, frequent switching between erosion and deposition occurs throughout the year, making the geomorphological system extremely dynamic and complex. Little knowledge of the impact of water impoundment on soil erosion in the DZ in the TGR is currently available. Although the limited results from previous studies have demonstrated that the depth of soil erosion varies spatially and its variation is dependent on altitude (Bao et al., 2015b; Su et al., 2017), it is still not clear how this depth changes from year to year. Hydrological, topographic, soil, geological and vegetation conditions are the critical factors that influence soil erosion (Vilmundardóttir et al., 2010; Bao et al., 2015b; Kaczmarek et al., 2016;). If the endogenic agency (i.e., vegetation and topography) and exogenic agency (i.e., frequent water level fluctuations, wave action from wind and boat traffic, and overland runoff) of soil erosion change over time, then we propose that there will be spatial-temporal variability in soil erosion followed by changes in environmental variables. In order to test this hypothesis, this study quantified the spatial and temporal changes in soil erosion in the DZ of the TGR using data collected from 2008 to 2016 through an extensive field survey and a nine-year in situ monitoring program around Zhong County, Chongqing Municipality in the middle of the TGR. This study aimed to understand the soil erosion trends at different spatial and temporal scales in the DZ of the TGR and provide first-hand information for future soil conservation planning in this zone.

2. Material and methods

2.1. Study area

The TGR covers a region of the Upper Yangtze River between

Chongqing and Yichang with a total water surface area of 1080 km^2 (Fig. 1). Following full impoundment in 2010 (Yang et al., 2012), the water level of the TGR rises to a maximum of 175 m during the dry season (October–March) every year and is used for energy generation. The water level then gradually drops to the base level of 145 m during the wet season (April–September) to enable flood control. The development of the TGR to the full storage capacity of 3.93 billion m^3 resulted in a DZ with a vertical height of 30 m and a total area of 349 km^2 along a 660 km reach from Yichang to the upstream section of Chongqing (Lu and Higgitt, 2001; Shao, 2008). Since this zone is subject to regular reservoir operations, its hydrological regime is characterized by annual cyclic water level variations combined with additional changes due to frequent rainfall during the wet season (Bao et al., 2015a). Thus, the magnitude and frequency of the reservoir flow in this zone are controlled by the dramatic change in the water level from 145 to 175 m during an annual cycle. This altered hydrological regime has triggered substantial environmental changes within the DZ (Zhang and Lou, 2011), including intensified soil erosion.

Morphologically, the DZ of the TGR includes three soil profiles (see Fig. 5 in Bao et al., 2015a). The first profile mainly comprises silt and clay on an approximately linear and gentle slope extending laterally for > 100 m. The second profile comprises soils and rock fragments on a slope with variable gradients that extend laterally no > 100 m. The third profile consists of a thin layer of underlying bare soils with carbonate and other bedrocks. The first profile type has been subject to the most intensive soil erosion and thus was the focus of this study. Specifically, the first DZ type located around Zhong County, Chongqing Municipality in the middle of the Upper Yangtze River was selected as the study area (30°24′–30°26′N, 108°08′–108°11′E) (Fig. 1). The climate of the study area is dominated by a humid subtropical monsoon climate with a mean annual precipitation varying from 886 to 1614 mm. A substantial proportion of the annual precipitation occurs during the wet season from May to September (Ye et al., 2012). The bed rock of the study area includes sandstones, siltstones, and mudstones of the Jurassic Shaximiao Group (J_2s) and is dominated by "purple soil", which includes fast-weathering Jurassic rocks with 18% clay, 30% silt, and 52% sand that are susceptible to erosion. Previously, the land where the TGR is located consisted of sloping dry farmland, paddy fields, and grassland; now it is mainly grassland and bare land. The DZ of the study area specifically refers to the banks that are affected by the water level fluctuations between 145 and 175 m. The new flow regime dominating this zone may be represented by a hydrograph with a blunt yet round top curve, a series of low-magnitude serrated curves near the bottom, and two very steep limbs (Fig. 2). The lower end of the ragged curves at the bottom of the hydrograph represents the lowest water level of 145 m, while the top irregular curve reflects the water level around the maximum of 175 m during the dry season. The multiple local peaks with variable magnitudes are mainly distributed along the bottom and near the falling limb, signifying the contributions of storm events to the reservoir during the wet season. The magnitudes of these peaks are much smaller than that of the peak of the main hydrograph, suggesting that the new flow regime is dominated by operation-controlled water level fluctuations. The original vegetation in the DZ was dominated by annuals such as *Setaria viridis*, *Digitaria ciliaris*, and *Leptochloa chinensis*, perennials such as *Cynodo dactylon*, *Hemarthria altissima*, and *Capillipedium assimile*, and woody plants such as *Ficus tikoua*, *Pterocarya stenoptera*, and *Vitex negundo*. However, the annual plants listed above became the dominant species after the area was flooded for the reservoir (New and Xie, 2008; Ye et al., 2013; Zhang et al., 2013).

2.2. Sampling design and data acquisition

The types of soil erosion in the study area are diverse and may be classified as rainfall-runoff erosion during the exposed wet season, wave erosion during the inundation period, and gravitational erosion, such as mass failure, caused by the rapid changes in hydrological

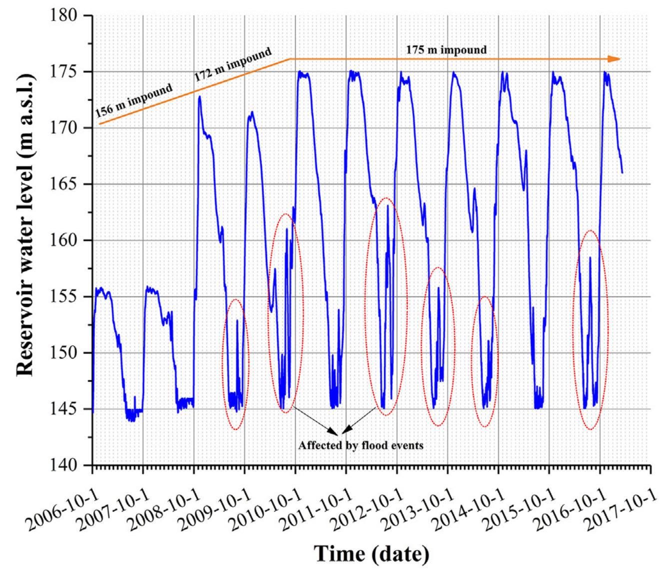

Fig. 2. The new hydrological regime in the Three Gorges Reservoir between 2006 and 2017. Orange circles showed the impact of rainfall on the hydrograph during the wet seasons.

conditions of hillslopes due to regular water level fluctuations. Therefore, erosion processes have a relatively high degree of spatial and temporal variability. To fully understand the variability, multiple monitoring methods are needed to capture the soil erosion rates over different short-term scales during a single rainfall event for both exposed and inundated periods. Thus far, methods based on remote sensing and topographic maps have been used to characterize soil erosion at larger spatial scales and over longer time frames (Gatto and Doe, 1987; Bayram et al., 2013; Bachofer et al., 2014). For example, Duru (2017) used remote sensing and geographical information system data to examine historical changes in the shoreline along Lake Sapanca from 1975 to 2016. However, the coarse scale of the aerial photography and satellite images and the obstruction by vegetation canopies can introduce a high degree of uncertainty to the estimated bank erosion rates (Day et al., 2013; Longoni et al., 2016). In recent years, a laser microtopographical scanner with high resolution has been used to quantitatively monitor dynamic river changes, define the riparian boundary, and estimate riverbank erosion (e.g., Lim et al., 2005; Rosser et al., 2005; Collins and Sitar, 2008; Kociuba et al., 2014). Unfortunately, this method is difficult to use when assessing erosion rates over short time frames because the equipment is expensive and suffers from accumulative errors from both multi-period comparisons and surface vegetation (Thorne, 1981; Nasermoaddeli and Pasche, 2008). Although new technologies have been developed to determine the continuous changes in soil erosion rates along river banks, such as the Photo Electronic Erosion Pin (PEEP) system (Lawler, 1991 & 2008; Papanicolaou et al., 2017), they can record only daytime data and tend to be more practical for single bank profiles than large areas. Erosion pins have been widely used in geomorphology since the 1950s to estimate the rates of soil erosion on land surfaces (e.g., Wolman, 1959; Vandekerckhove et al., 2001; Ghimire et al., 2013). Typically erosion pins measurements are taken once every year, or every month (Zaimes et al., 2017). It is common practice to calculate annual erosion rates from pin measurements as the mean net change in pin height over a given area, but some studies have found that there are some incongruence between erosion rates estimated from pins and other methods (Hancock and Evans, 2010; Hancock and Lowry, 2015). Kearney et al. (2018) suggest that when using erosion pins for monitoring changes in erosion over time, the absolute value of pin height change is likely a better indicator than net real number change. Although there are some doubts about the accuracy of the erosion pins approach, many studies have been more optimistic regarding measurement uncertainty (Boardman et al., 2015). Several studies report that the accuracy of erosion pin measurements is ± 0.5–1 mm (Benito et al., 1992; Sirvent et al., 1997). Hence, sites with low rates of erosion may not be suitable for erosion pin techniques because of measurement error. In addition, it is suggested that the disturbance of erosion pins by some natural processes (i.e., frost heave, swelling, collapse and creep of soils) need to be took into account when the erosion pins are installed and measured (Boardman and Favis-Mortlock, 2016). In summary, the use of erosion pins for quantifying short-term erosion rates is still suitable for field observations because they not only are cost-effective and easy to operate but also may be used for larger areas (Simon et al., 1999; Couper et al., 2002; Stott, 2005; Harden et al., 2009; Vietz et al., 2017; Rando et al., 2017). Furthermore, the relatively short distances between pins help avoid the potential impact of surface vegetation on measurement accuracy. For these reasons, we used erosion pins to observe the spatial and temporal changes in soil erosion rates from 2008 to 2016.

Field measurements were taken in two DZs stretching 8 km along the mainstream of the Upper Yangtze River and 3 km along the Ruxi River, which is a first-order tributary of the Upper Yangtze River. Nine transects were selected along the lateral direction of the DZ in the mainstream (M1–M9). M1 was the most downstream transect, while M9 was the most upstream one. Three transects were chosen in the tributary and labeled T1–T3 from downstream to upstream, respectively. Each transect was 10 m wide (parallel to the flow direction) with a variable length of at least 100 m (perpendicular to the flow direction) and was located between the minimum (145 m) and maximum (175 m) water levels of the reservoir. Each transect included three rows of erosion pins with approximately equal spacing between rows. These transects contained a variety of soil types, land types, topography and vegetation and, thus, were representative of the study area (Table 1).

Within each transect, metallic and plastic erosion pins with a fixed length of 60 cm were installed 1 m apart from each other. The top 10 cm of the pin were above the ground. To assure the quality of the data, we kept the soil disturbance to a minimum during installation. Transects M3, M9 and M2 were longer than the others and contained 450, 375 and 330 pins, respectively. The remaining nine transects contained between 270 and 300 pins. A total of 2850 and 870 erosion pins were installed in the mainstream disturbance zone and tributary disturbance zone (MDZ and TDZ), respectively (Table 2). From August 2007, when the reservoir water level was lowered, these pins were measured and inspected annually. The exposed length of an erosion pin reflects the time-integrated changes in surface micro-topography caused by soil erosion/deposition between measurements.

Soil erosion in the DZ of the TGR is highly dynamic, and its magnitude should be sensitive to different events. However, steps of water impoundment with increasing magnitude and seasonal water level fluctuations have created interannual variations in the hydrological regime, which have become a principal factor in determining soil erosion in the DZ. Thus, measurements of the annual soil erosion rate corresponding to the changing hydrological regime can help explain how soil erosion evolves and determine its temporal pattern with consistent operation of the Three Gorges Dam. Furthermore, from a practical view, event-based measurements of soil erosion are challenging and difficult due to the frequent water level fluctuations in the summer season and the long flooding durations in the winter season. Hence, the observing program utilizes one year as the measurement unit. That is, each erosion pin is measured and recorded using a rigid steel ruler once each year according to the rhythm of reservoir water level fluctuations. The annual soil erosion rate is calculated by comparing the measured values with values observed in the previous year. Details on the methods used to determine the soil erosion rate ($t \cdot yr^{-1}$) may be found in Bao et al. (2015b).

The change in soil erosion rate over two consecutive years (Q) may be calculated as follows:

$$Q = S_i - S_{i+1} \tag{1}$$

where S_i is the soil erosion rate at year i, and S_{i+1} is the erosion rate at year i + 1. A positive or negative value of Q indicates a decrease or increase in the soil erosion rate, respectively. The altitude of each erosion pin was measured by combining the value obtained using an altimeter with 1 m accuracy with the recorded real-time water level. The water level was directly read from the reservoir staff gage (approximately 1 km upstream of the study area). Daily water levels of the reservoir at the outlet were downloaded from the website of the China Three Gorges Corporation (http://www.ctgpc.com.cn). The water level fluctuation schedule is shown in Fig. 2. Using these data, the flooding duration at different altitudes was calculated.

t-Test analysis and analysis of variance (ANOVA) are statistical methods that are widely used for judging whether group means are

Table 1
Characteristics of the sampling transects along the mainstream and tributary disturbance zones (MDZ and TDZ).

Sites	No.	Coordinates	Soil type	Vegetation	Slope morphology	Slope gradient
MDZ	M1	30°25′15.9″N 108°10′30.3″E	Purple soil	Crop, Natural meadow, average vegetation coverage is range from 10% to 86%	Slope + terrace	5°–20°
	M2	30°25′15.6″N 108°10′24.9″E	Purple soil	Natural meadow, average vegetation coverage is range from 20% to 60%	Slope + terrace	2°–15°
	M3	30°25′03.4″N 108°9′55.9″E	Purple soil	Crop, Natural meadow, average vegetation coverage is range from 25% to 70%	Slope + terrace	2°–10°
	M4	30°24′58.1″N 108°9′46.2″E	Purple soil	Natural meadow, average vegetation coverage is range from 20% to 90%	Slope + terrace	10°–36°
	M5	30°24′53.4″N 108°9′32.7″E	Purple soil	Natural meadow, average vegetation coverage is range from 20% to 90%	Slope + terrace	5°–38°
	M6	30°24′48.5″N 108°9′16.2″E	Purple soil	Natural meadow, average vegetation coverage is range from 20% to 70%	Slope + terrace	10°–30°
	M7	30°24′23.5″N 108°8′47.7″E	Purple soil	Natural meadow, average vegetation coverage is a range from 25% to 80%	Slope + terrace	10°–22°
	M8	30°24′20.8″N 108°8′41.1″E	Purple soil	Natural meadow, average vegetation coverage is a range from 0% to 35%	Slope	5°–38°
	M9	30°24′15.5″N 108°8′28.5″E	Purple soil	Crop, Natural meadow, average vegetation coverage is range from 20% to 90%	Slope + terrace	2°–15°
TDZ	T1	30°24′22.27″N 108°8′46.25″E	Purple soil	Natural meadow, average vegetation coverage is range from 20% to 90%	Slope + terrace	2°–20°
	T2	30°24′57.47″N 108°8′44.44″E	Purple soil	Natural meadow, average vegetation coverage is range from 20% to 80%	Slope + terrace	5°–25°
	T3	30°25′33.12″N 108°8′34.61″E	Purple soil	Natural meadow, average vegetation coverage is range from 30% to 95%	Slope + terrace	2°–15°

Table 2
Design of erosion pins in the sampling transects.

Sites	No.	Coordinates	Slope length (m)	Number of pins	Slope gradient (°)*			Vegetation cover (%)		
					Lower	Middle	Upper	Lower	Middle	Upper
MDZ	M1	30°25′15.9″N 108°10′30.3″E	100	300	10–20	5–15	15–20	20–30	10–50	30–86
	M2	30°25′15.6″N 108°10′24.9″E	110	330	10–15	2–10	10–15	20–35	30–50	50–60
	M3	30°25′03.4″N 108°9′55.9″E	150	450	5–10	2–10	5–10	25–35	40–60	60–70
	M4	30°24′58.1″N 108°9′46.2″E	95	285	10–36	10–15	15–36	20–30	20–50	50–90
	M5	30°24′53.4″N 108°9′32.7″E	95	285	10–35	5–15	20–38	20–30	25–65	50–90
	M6	30°24′48.5″N 108°9′16.2″E	90	270	10–30	15–30	20–30	20–30	40–60	60–70
	M7	30°24′23.5″N 108°8′47.7″E	95	285	10–22	10–22	10–22	25–35	30–60	60–80
	M8	30°24′20.8″N 108°8′41.1″E	90	270	15–38	10–25	20–38	0–10	0–10	10–35
	M9	30°24′15.5″N 108°8′28.5″E	125	375	2–15	10–15	10–15	20–45	30–75	40–95
TDZ	T1	30°24′22.27″N 108°8′46.25″E	95	285	2–15	10–20	10–20	20–35	30–65	50–90
	T2	30°24′57.47″N 108°8′44.44″E	95	285	5–15	5–25	15–22	20–45	30–50	50–80
	T3	30°25′33.12″N 108°8′34.61″E	100	300	2–10	2–10	10–15	30–50	40–75	60–95

* The topographic position of each transect hillslope is divided into three categories from the ridge tops (175 m altitude) to the bottoms (145 m altitude): lower, middle, and upper slope. The lower slope is the area toward the base of the slope. The middle slope is the area between the upper and lower slopes. The upper slope is the upper portion immediately below the crest of 175 m water level.

statistically similar or not (Kao and Green, 2008). The former analyses the means for two groups, while the latter analyses the means of more than two groups (Kim, 2014). In this study, the *t*-test method was used to examine the difference in the annual soil erosion rates between the MDZ and TDZ and the (one-way) ANOVA method was adopted to evaluate the differences of these rates among different monitoring locations and different years. All statistical analyses were carried out at the 95% confidence level (i.e., $p < 0.05$). In addition, four different commonly used regression models (i.e., linear, power, exponential and polynomial) (Liu et al., 1994; Jin, 1996; Nunes et al., 2011; Suleman et al., 2014) were developed to capture the relationship between annual erosion rates and each of the two relevant variables, local slope and percentage vegetation cover within the study area.

3. Results

3.1. Intensity of soil erosion

From the 12 sampling transects in the studied DZ, the observed maximum value of the mean annual erosion depth between 2008 and 2016 was 48 mm at M5, and the minimum value was 5 mm at T3 (Table 3). The mean annual erosion depth ranged from 22 to 48 mm in the MDZ, with an average of 37 mm, while it ranged from only 5 to 7 mm with an average of 6 mm in the TDZ. Spatially, the annual eroded soil depth showed apparent heterogeneity along each transect. The maximum and minimum values of individual soil erosion depths were 115 and 1 mm, respectively. The annual eroded soil depths of the nine transects in the MDZ had standard deviations varying from 10.6 to 18.5 mm during the study period (i.e., 2008–2016), while those for the three transects in the TDZ ranged from 1.1 to 1.3 mm. The coefficient of variance (CV) ranged from 28.8% to 57.8% in the MDZ, but it ranged from 23.1% to 25.3% in the TDZ. Specifically, the CV of soil erosion depth for the M9 transect in the MDZ was the largest (57.8%), while the T1 transect in the TDZ had the lowest CV value (23.1%). The CV values of soil erosion depth for the different transects in the TDZ were significantly lower than those in the MDZ (*t*-test, $p = 0.016$). However, the CV values for soil erosion depth in the MDZ were approximately one to three times greater than those in the TDZ. These results indicate that soil erosion rates were highly spatially variable, with a higher degree of variation in the MDZ.

Following the same trend, the mean annual erosion rate ranged from 32,383 to 69,593 $t\,km^{-2}\,yr^{-1}$ when the site-specific bulk density was considered, with an average of 54,050 $t\,km^{-2}\,yr^{-1}$ in the MDZ, whereas this value varied from 8107 to 10,360 $t\,km^{-2}\,yr^{-1}$, with an average of 9191 $t\,km^{-2}\,yr^{-1}$ in the TDZ (Table 3). Evidently, the rate of soil erosion was significantly higher in the MDZ than that in the TDZ (*t*-test, $p = 0.0001$), and the mean annual erosion rate of the former was > 6 times higher than that of the latter.

3.2. Variability of soil erosion rates at different elevations

The 12 transects may be roughly grouped into four categories according to their physiographic properties (i.e., slope length, slope gradient and vegetation). The first group included M1 and M2, which were 100 m long with relatively shallow gradients. The second group included M3 and M9, which were covered with crops and natural meadows; they were approximately 125 m long with the lowest gradients. The third group contained M4, M5, M6, M7 and M8, which had steeper gradients and shorter slope lengths. The last group included T1, T2 and T3, which were located in the TDZ and were approximately 100 m long. Fig. 3 shows the relationship between the annual soil erosion rates from 2008 to 2016 and the altitudes associated with these four transect types in the study area. The range of soil erosion rates between 145 and 175 m altitude (i.e., M1, M6 and M9 in Fig. 3; all altitudes quoted in this paper are meters above sea level) was generally larger along transects in the MDZ than that in the TDZ, suggesting that soil erosion was more dynamic in the MDZ. In addition, the soil erosion rates at all altitudes displayed distinct patterns in the transects between the MDZ and TDZ. The erosion rates in the MDZ generally decreased from 145 to 150 m altitude and then fluctuated from 150 to 175 m with different magnitudes of fluctuation at different ranges of elevations and along different transects (Fig. 3). From 150 to 168 m altitude, the overall trends of the

Table 3
Statistical properties of soil erosion depths and rates in the disturbance zone (DZ) of the study area (2008–2016).

Sites	No.	Coordinates	Annual erosion depth					Bulk density (g cm^{-3})	Annual erosion rate (t·km^{-2}·yr^{-1})
			Mean (mm)	Minimum (mm)	Maximum (mm)	Standard deviation	CV (%)		
MDZ	M1	30°25′15.9″N 108°10′30.3″E	43	5	110	18.5	44.3	1.41	60,787
	M2	30°25′15.6″N 108°10′24.9″E	31	5	70	11.5	39.6	1.45	44,628
	M3	30°25′03.4″N 108°9′55.9″E	28	5	65	10.4	39.0	1.47	40,670
	M4	30°24′58.1″N 108°9′46.2″E	44	10	95	12.4	28.8	1.49	65,394
	M5	30°24′53.4″N 108°9′32.7″E	48	1	115	13.9	30.2	1.46	69,593
	M6	30°24′48.5″N 108°9′16.2″E	40	4	85	13.0	34.3	1.49	59,931
	M7	30°24′23.5″N 108°8′47.7″E	39	2	92	13.7	38.6	1.46	56,940
	M8	30°24′20.8″N 108°8′41.1″E	38	1	85	12.9	36.9	1.49	56,123
	M9	30°24′15.5″N 108°8′28.5″E	22	1	65	10.6	57.8	1.45	32,383
TDZ	T1	30°24′22.27″N 108°8′46.25″E	6	1	15	1.2	23.1	1.49	9106
	T2	30°24′57.47″N 108°8′44.44″E	7	1	19	1.3	23.4	1.48	10,360
	T3	30°25′33.12″N 108°8′34.61″E	5	1	15	1.1	25.3	1.52	8107

erosion rates at M1 and M9 were similar, peaking at the altitudes of 155 and 165 m, respectively. However, for the remaining elevations, two different trends can be identified. After a rapid increase from 168 to 172 m altitude, the erosion rate at M1 decreased gradually from 172 to 175 m altitude, whereas there was a steady increase from 168 to 175 m altitude at M9. By contrast, there was little change at M6 from 150 to 155 m altitude. After reaching the lowest value at an altitude of 158 m, the erosion rate increased again from 160 to 165 m, and then decreased from 165 to 170 m. Finally, the erosion rate increased from 170 to 175 m altitude. At the transect T3 in the TDZ, the erosion rate decreased slightly from 145 to 150 m altitude, which subsequently remained constant up to 160 m and then increased gradually up to the 175 m

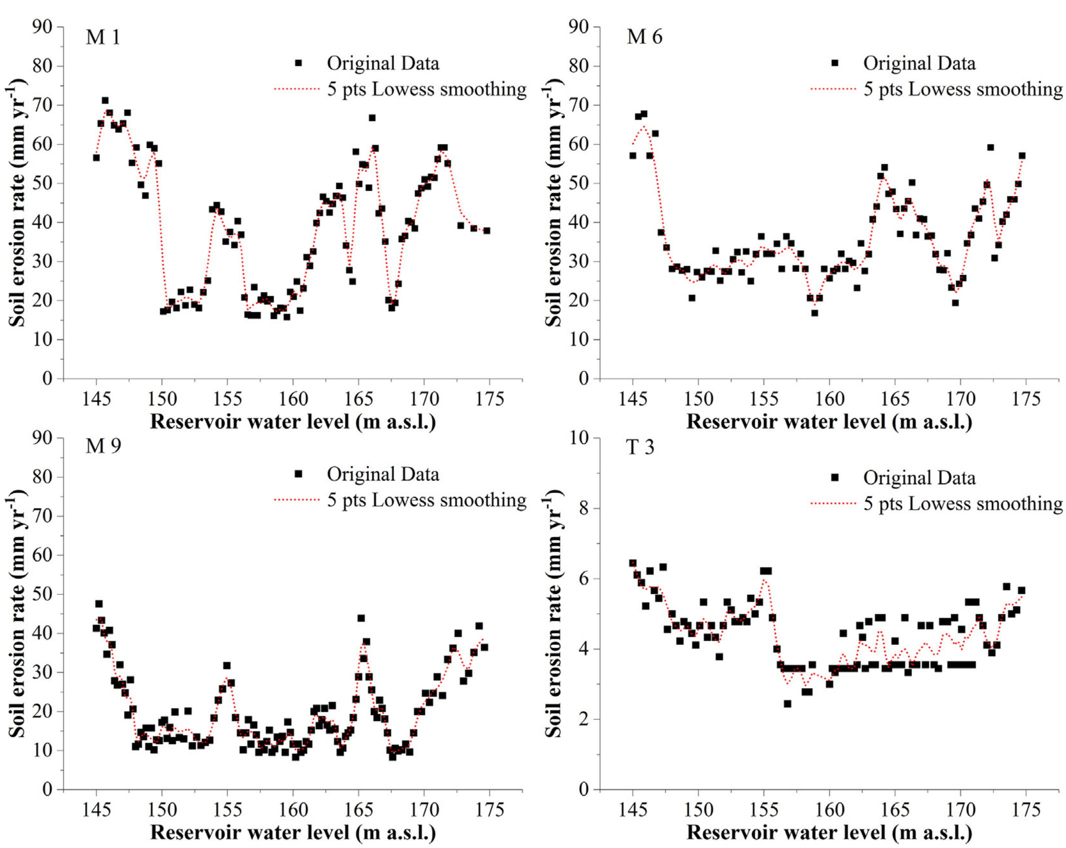

Fig. 3. Soil erosion rate versus elevation at four typical transects in the study area between 2008 and 2016.

Table 4
Comparison of soil erosion rates in the study area between the mainstream and tributary disturbance zones (MDZ and TDZ).

Sites	Elevation (m a.s.l.)	On each transect ($mm\,yr^{-1}$)*
MDZ	145–150	35.0 ± 15.8d
	150–155	26.4 ± 7.6b
	155–160	23.8 ± 8.9a
	160–165	34.4 ± 12.8cd
	165–170	31.7 ± 11.2c
	170–175	42.0 ± 10.8e
Average	145–175	32.0 ± 13.1a
TDZ	145–150	5.9 ± 0.8c
	150–155	5.7 ± 0.9c
	155–160	4.1 ± 0.8a
	160–165	4.8 ± 0.9b
	165–170	4.9 ± 1.0b
	170–175	5.5 ± 0.9c
Average	145–175	5.1 ± 1.1b

* The results are given as the mean ± SD. Values in the same column followed by different letters indicate significant differences at significance level of 0.05.

altitude (Fig. 3). Again, the higher elevation-related vertical variation of the soil erosion rates along the nine transects in the MDZ suggests that soil erosion processes were more dynamic in the MDZ than in the TDZ.

The annual mean soil erosion rate from all transects in the MDZ was 32.0 $mm\,yr^{-1}$. At altitudes of 170–175 m, 145–150 m and 160–165 m, the annual mean soil erosion rates were higher than the mean with values of 42.0, 35.0 and 34.4 $mm\,yr^{-1}$, respectively. However, at altitudes of 165–170 m, 150–155 m and 155–160 m, the erosion rates were lower than the mean with values of 31.7, 26.4 and 23.8 $mm\,yr^{-1}$, respectively (Table 4). Overall, the zone at the altitudes of 170–175 m experienced more intensive erosion than that at altitudes of 145–170 m, followed by the erosion rates at altitudes of 145–150 m, 160–165 m and 165–170 m (one-way ANOVA, $p < 0.05$).

Nonetheless, there were much smaller elevation-based variations in the erosion rates for the TDZ (Table 4). The annual average soil erosion rate for all three transects was only 5.1 $mm\,yr^{-1}$. Within the 145–150 m, 150–155 m and 170–175 m altitude ranges, it was 5.9, 5.7 and 5.5 $mm\,yr^{-1}$, respectively, with no significant difference between these altitude ranges (one-way ANOVA, $p > 0.05$). The annual soil erosion rates for the altitudes of 160–165 m and 165–170 m were 4.9 and 4.8 $mm\,yr^{-1}$, respectively, so slightly lower than the mean. All transects in the TDZ that were in the altitude range 155–160 m had the lowest annual soil erosion rate, which was 4.1 $mm\,yr^{-1}$. However, the soil erosion rates for the 145–155 m and 170–175 m altitude ranges were greater than those for the 160–170 m and 155–160 m altitude ranges (one-way ANOVA, $p < 0.05$).

3.3. Temporal variation of soil erosion

The average soil erosion rates of the 12 transects in different years ranged from 15 to 50 $mm\,yr^{-1}$ for the MDZ and from 1 to 15 $mm\,yr^{-1}$ for the TDZ (Fig. 4). During the nine-year study period (2008–2016), the soil erosion rates decreased gradually for all transects in both the MDZ and TDZ with the highest values in 2008 and the lowest in 2016 (Fig. 4). There were also obvious and large interannual variations, which were most easily observed in the 5-point locally weighted scatterplot smoothing (LOWESS) regression curve (Fig. 4). These results showed that the soil erosion rate was negatively correlated with time at all transects, and the polynomial model fitted the data the best for all transects in both the MDZ and TDZ.

The average annual rate of change (Q in Eq. (1)) in soil erosion at all transects in the MDZ was 4.1 $mm\,yr^{-1}$, whereas it was only 1.7 $mm\,yr^{-1}$ at the transects in the TDZ. This value in the MDZ was

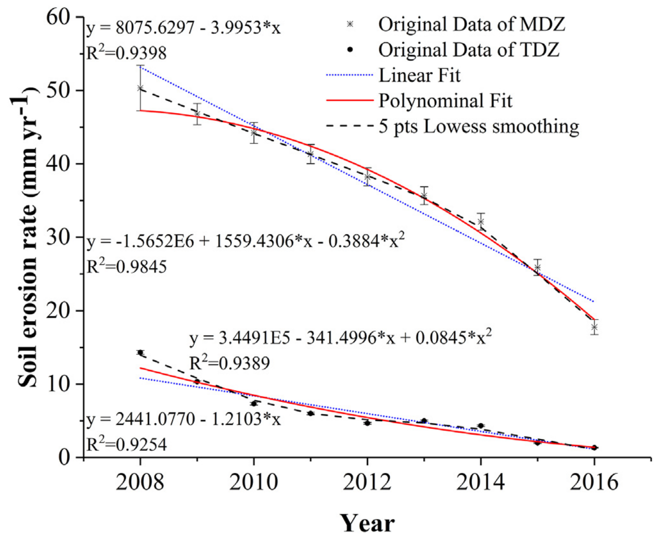

Fig. 4. Inter-annual variation of the soil erosion rates at different transects of the study area from 2008 to 2016.

Table 5
Rates of change of annual soil erosion (i.e., Q) in the mainstream and tributary disturbance zones (MDZ and TDZ).

Sites	Year	Q (mm)		One-way ANOVA
		Maximum	Minimum	Inter-annual*
MDZ	2009	7	2	3.6 ± 1.7a
	2010	4	1	2.6 ± 0.9a
	2011	5	1	2.9 ± 1.4a
	2012	6	0	3.1 ± 2.0a
	2013	6	0	2.6 ± 1.7a
	2014	6	1	3.6 ± 1.5a
	2015	8	5	6.2 ± 1.0b
	2016	15	3	8.1 ± 3.5c
	Total	15	0	4.1 ± 2.6a
TDZ	2009	5	3	4.0 ± 1.0d
	2010	3	3	3.0 ± 0.4 cd
	2011	2	1	1.3 ± 0.6ab
	2012	3	0	1.3 ± 1.5ab
	2013	1	0	0.3 ± 0.6a
	2014	1	0	0.7 ± 0.6a
	2015	3	2	2.3 ± 0.6bc
	2016	1	0	0.7 ± 0.6a
	Total	5	0	1.7 ± 1.4b

* The results are given as the mean ± SD. Values in the same column followed by different letters indicate significant differences at significance level of 0.05.

statistically higher than that in the TDZ (one-way ANOVA, $p < 0.05$). This value was also statistically similar among the transects of the MDZ over the study period (2008–2014). The value of Q was, however, significantly higher in 2015 and 2016 than in the other years (Table 5), when the Q values were 6.2 and 8.1 $mm\,yr^{-1}$, respectively. While the rate of change (Q) in annual soil erosion from 2008 to 2014 ranged from 2.6 $mm\,yr^{-1}$ to 3.6 $mm\,yr^{-1}$, which is slightly lower than the average (Table 5), it was significantly different from the rates at the transects in the TDZ during the initial period (2008–2009) with values of 4.0 and 3.0 $mm\,yr^{-1}$. After 2009, this value decreased linearly for all transects in the TDZ.

4. Discussions

4.1. Effect of the altered hydrological regime on soil erosion

Soil erosion in any reservoir or lake DZ is an important factor that

Table 6
Soil erosion rates in the disturbance zone (DZ) of many reservoirs and lakes and the hillslope above the DZ of the TGR.*

Location	Land use	Gradient (°)	Erosion rates		Data source	Methods
			($t\,km^{-2}\,yr^{-1}$)	($mm\,yr^{-1}$)		
Sloping land of the Upper Yangtze River area	Annual culture	6	3122		Zhu et al., 2002	Erosion pins
	Annual culture	15	4969		Jiang and Li, 1995	Runoff plots
Sloping land of the TGR	Annual culture	24	2965		Jing and Zhang, 2007	Runoff plots
	Shrub and grassland	25	933			
	Bare land	23	2970			
	Bare land	33	4961			
	Annual culture	24	3750		Dong, et al., 2009	Runoff plots
	Grassland	10	2330		Shi et al., 2011	Erosion pins
DZ of TGR	Artificial grassland	15	21,340	15	Bao et al., 2012	Erosion pins
	Natural grassland	15	37,794	26		
	Bunch planting	15	64,670	41		
	Annual culture	15	94,887	59		
	Bare land	15	92,423	55		
	Natural Grassland	15.6	32,625	23	Su et al., 2017	Erosion pins
	Natural Grassland	15.9	9280	6		
	Natural Grassland	19.3	12,180	8		
	Natural Grassland	24	10,150	7		
DZ of Itaipu reservoir	Annual culture	Cutbank (> 50°)		620	Fernandez and Fulfaro, 2000	Erosion pins
	Afforestation			670		
	Grassland			1630		
DZ of Flathead lake	Bareland	Cutbank (> 50°)		500–2500	Lorang and Stanford, 1993	Erosion pins
DZ of Porto Primavera Reservoir	Bareland	Cutbank (20–30° or Bluff)		958–6417	Siqueira et al., 2015	Bathymetric surveys

* These data were obtained using three different methods, erosion pin, runoff plot, and bathymetric survey, each of which has limitations in accuracy and reliability (Hudson, 1993). Nonetheless, they are all based on direct in situ observation and may give rise to annual surface erosion rates (Li et al., 1995). Furthermore the potential errors due to their limitations are much less than the difference of the measured erosion rates among different reservoirs, as well as between the DZ and its above hillslope of the TGR. Thus, these data are comparable.

controls the morphological changes in reservoirs or lake banks. The annual soil erosion depths in the DZs of other reservoirs and lakes around the world may be two orders of magnitude higher than those in the DZ of the TGR (Table 6). This vast difference in soil erosion rate between the two must reflect their different morphological processes. The DZs in the former are indeed banks that have heights that range from only 0.5 to 12 m and slopes varying from 20° to almost vertical (i.e., cliffs). Their soil erosion rates were measured as either the depth of soil accumulation at the bank toe or the rates of bank recession (Siqueira et al., 2015). Thus, these measurements are essentially the rates of mass wasting processes. In the TGR, however, the banks of the DZ are gently sloped and long, and thus, the measured rates are the true surface soil erosion rates, which should be, in principle, much less than those necessary for bank collapse. The difference in morphology between the DZs of other reservoirs (and lakes) and that of the TGR also suggests that the latter is unique (Bao et al., 2015a) and deserves more attention.

Within the TGR, soil erosion rates in the DZ can be 20 times higher than those on the steep uplands above the DZ (Table 6). The latter area are located at altitudes above 175 m where erosion is solely controlled by natural hydrological processes, whereas erosion in the former area is dominated by the combination of (i) the artificially regulated hydrological regime that is characterized by an annual cycle of flooding and draining, and (ii) the natural hydrological processes due to summer rainfall events. Therefore, the morphology of the DZ in the TGR is shaped by both aquatic processes due to oscillatory flows (i.e., flows driven by surface waves) and terrestrial, fluvial processes due to storm flows (Bao et al., 2015a).

The magnitude of soil erosion in the DZ of the TGR not only varies spatially due to locally variable hydrological and morphological conditions but also demonstrates high inter-event variability that is mainly controlled by flood characteristics and the cycle of reservoir water level regulation (Nagle et al., 2012; Kronvang et al., 2013; Bao et al., 2015a). Furthermore, the timing (i.e., season), duration, frequency, rate of change, and magnitude of water impoundment have been identified as important factors for characterizing the geomorphological and ecological processes within the DZ (Nilsson and Svedmark, 2002; Bao et al., 2015a). Our previous studies showed that the variations and magnitudes of water waves in the mainstream were significantly higher than those in the tributary (Bao et al., 2015b; Li et al., 2016), which may be the main reason for the mean annual erosion rates in the MDZ generally being more than six times higher than those in the TDZ.

Our findings also indicated that soil erosion markedly fluctuated with altitude in the DZ of the TGR. This elevation-dependent pattern of soil erosion may be caused by the altered hydrological regime resulting from the water in the reservoir together with variable flows due to surface waves. As shown in Fig. 5, the fluctuation pattern of soil erosion rates in the DZ was consistent with that of the specific water level residence time. The residence times around the minimum and maximum levels were significantly longer than those at the other levels. The lower the altitude, the longer it took for the associated DZ to be flooded over a one-year cycle.

4.2. Effects of slope and vegetation on dynamic changes of soil erosion

Slope gradient is essential variables that control soil erosion on hillslopes due to overland flow (Liu et al., 2001). As the slope gradient increases, the amount of soil loss increases when the surface roughness remains unchanged (Fang et al., 2014). Thus, a statistically significant relationship between the slope and the associated soil erosion rate should exist. A regression analysis using four different models (Fig. 6) showed that the soil erosion rate was positively correlated with the slope gradient in general, which was consistent with the hydraulic principle. A comparison of the models indicated that the polynomial and exponential models fitted the data better than the linear and power models for both grassland and bare land. However, the power model still performed well (Fig. 6). In particular, the power model captured the curved trends of the measured data. Given that the power model requires fewer coefficients than either the polynomial or exponential model, it would have a lower degree of uncertainty than those of the

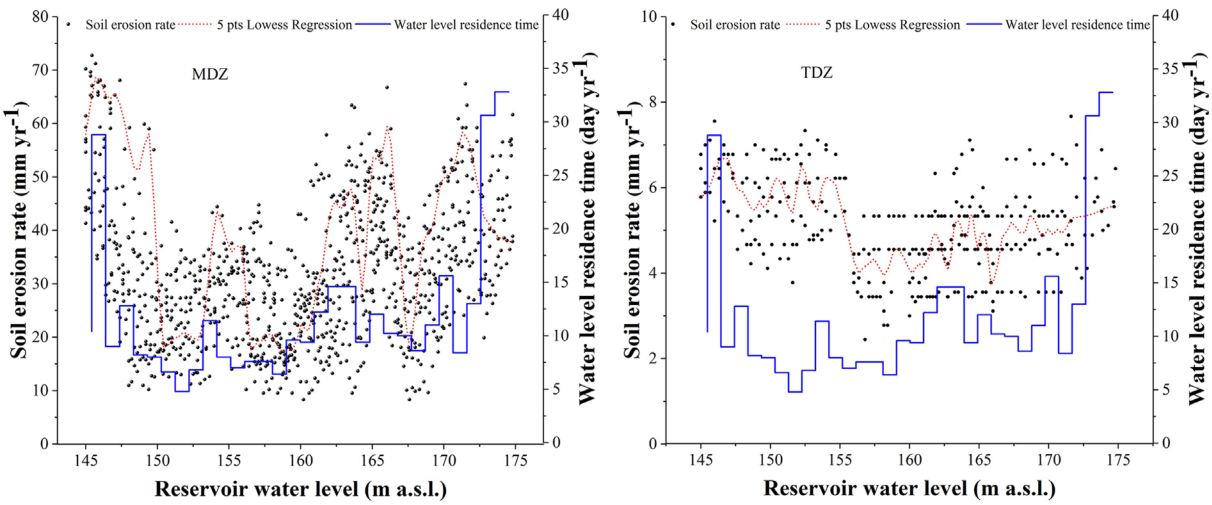

Fig. 5. The annual average residence periods at different water levels and the associated soil erosion rates within the study area.

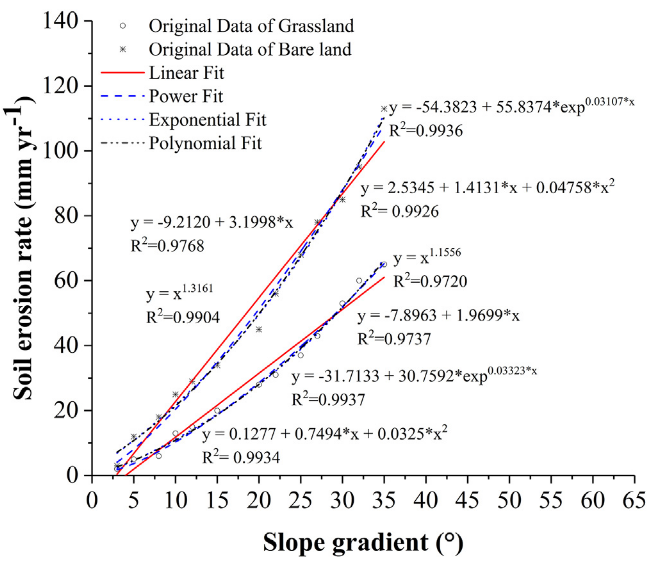

Fig. 6. Four regression models for the relationship between soil erosion rate and slope gradient in the grassland and bare land.

other two models when used for prediction. Therefore, the power model may be used in the future to characterize the possible changes in these relationships.

In addition to slope gradient, vegetation may also significantly affect erosion in the DZ of the TGR (Coops et al., 1996; Simon and Collison, 2002; Wynn and Mostaghimi, 2006; Zuazo and Pleguezuelo, 2008; Du et al., 2010). A dense vegetation cover reduces the possibility of soil being disturbed by raindrops, runoff and reservoir water waves. Vegetation may also bind surface soil using its roots and hence increase soil resistance to erosion. These two roles of vegetation explained the finding that soil erosion rate decreased as vegetation cover increased over all slope gradients (Fig. 7a). When the soil erosion rates for different slope gradients were averaged for a given vegetation cover, the relationship between the averaged rates and the associated vegetation cover could be shown with an exponential model (Fig. 7b), suggesting that in the DZ of the TGR, the impact of vegetation was higher than that of slope on soil erosion.

Since the TGR reached full operation in 2010, the reservoir has created a new annual hydrological regime that regularly switches between wet and dry seasons (Fig. 2). Consequently, the vegetation in the DZ of the TGR has been subject to seasonally variable flows and cycles of wet and dry seasons (New and Xie, 2008; Bao et al., 2015a). Influenced by this new hydrological regime, the abundance of the original plant species within the DZ has been drastically reduced (Huang, 2001; New and Xie, 2008); in particular, this reduction rate was high at the beginning of the new hydrological regime and decreased gradually thereafter (Zhu et al., 2015). After the initial period (approximately two or three years), vegetation in the DZ began to gradually adapt to the new environment. Some species that could handle different flooding periods at different elevations survived. This adjustment catalyzed the development of a new vegetation trend that exhibited an elevation-dependent gradient of vegetation distribution in the DZ of the TGR (Wang et al., 2011; Wang et al., 2012). Furthermore, the vegetation recovery rate in the TDZ is higher than that in the MDZ, and the vegetation coverage in the former is much higher than that in the latter (Chinese academy of engineering, 2014). This partial recovery could reduce the degree of soil erosion. Furthermore, morphological changes in the topography of the DZ have caused a gradual reduction in its slope gradient (Bao et al., 2010; Chinese academy of engineering, 2014; Bao et al., 2015b; Su et al., 2017). These changes in vegetation and slope gradient might continue and will play an important role in reducing soil erosion in the DZ of the TGR.

5. Conclusions

The geomorphological adjustment of the DZ of China's TGR is in its early stages. Understanding the processes that control soil erosion in this zone is an emerging new research topic. This study reported the soil erosion rates obtained through extensive field measurements and in situ monitoring between 2008 and 2016. However, it is still unknown exactly how long before the soil erosion rate becomes stable or approaches zero. Continuous large-scale and long-term monitoring and surveying are required to understand the explicit trends in soil erosion. Furthermore, process-based erosion models and new sampling strategies should be developed to characterize the relative magnitudes of soil erosion rates at different elevations of the MDZ and TDZ, which will allow for the identification of the relative importance of different factors acting on the DZ of the TGR. The results from this study suggest that conservation actions should be mainly targeted at mainstream reaches, especially for sections with elevations < 155 m or > 170 m, where significant soil erosion has been observed. Vegetation restoration is a major strategy that can reduce soil erosion, improve landscapes, as well as enhance ecosystem values and services.

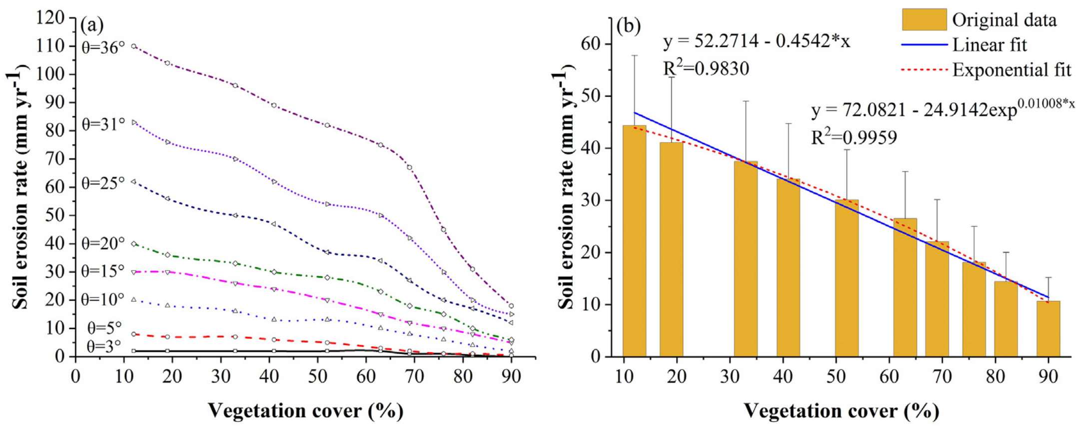

Fig. 7. Soil erosion rate versus vegetation cover for different slope gradients. (a) Soil erosion rate under different slope gradients and vegetation cover; (b) slope-averaged relationship between soil erosion rate and vegetation cover.

Acknowledgements

Financial support for this study was jointly provided by the National Natural Science Foundation of China (grant nos. 41571278, 41771320 and 41771321), Sichuan Science and Technology Program (2018SZ0132), and the program of China Scholarship Council. Qiang Tang is supported by a UK Royal Society Newton International Fellowship scheme.

References

Anbumozhi, V., Radhakrishnan, J., Yamaji, E., 2005. Impact of riparian buffer zones on water quality and associated management considerations. Ecol. Eng. 24, 517–523.
Avakyn, A.B., 1975. Problems of creating and operating reservoirs. Soviet Hydrol. 3, 149–199.
Bachofer, F., Quénéhervé, G., Märker, M., 2014. The delineation of paleo-shorelines in the Lake Manyara basin using TerraSAR-X data. Remote Sens. 6 (3), 2195–2212.
Bao, Y.H., Nan, H.W., He, X.B., Long, Y., Zhang, X.B., 2010. Sedimentation in the riparian zone of the three gorges reservoir, China. IAHS Publ. 337, 221–225.
Bao, Y.H., He, X.B., Wei, J., Tang, Q., Guo, F., 2012. Soil erosion under different land uses in the riparian zone of the Three Gorges Reservoir, China. IAHS Publ. 356, 198–201.
Bao, Y.H., Gao, P., He, X.B., 2015a. The water-level fluctuation zone of Three Gorges Reservoir—a unique geomorphological unit. Earth-Sci. Rev. 150, 14–24.
Bao, Y.H., Tang, Q., He, X.B., Hu, Y.H., Zhang, X.B., 2015b. Soil erosion in the riparian zone of the Three Gorges Reservoir, China. Hydrol. Res. 46 (2), 212–221.
Bayram, B., Seker, D.Z., Acar, U., Yuksel, Y., Guner, A.A., Cetin, I., 2013. An integrated approach to temporal monitoring of the shoreline and basin of Terkos lake. J. Coast. Res. 29 (6), 1427–1435.
Benito, G., Gutierrez, M., Sancho, C., 1992. Erosion rates in badland areas of the central Ebro basin (NE-Spain). Catena 19, 269–286.
Boardman, J., Favis-Mortlock, D., 2016. The use of erosion pins in geomorphology. In: Cook, S.J., Clarke, L.E., Nield, J.M. (Eds.), Geomorphological Techniques. British Society for Geomorphology, London, UK (Online Edition).
Boardman, J., Favis-Mortlock, D., Foster, I., 2015. A 13-year record of erosion on badland sites in the Karoo, South Africa. Earth Surf. Process. Landf. 40 (14), 1964–1981.
Born, S.M., Stephenson, D.A., 1973. Water management of shoreline erosion control in the Chippewa Flowage. J. Soil Water Conserv. 27, 57–61.
Buckler, W.R., Winters, H.A., 1983. Lake Michigan bluff recession. Ann. Assoc. Am. Geogr. 73 (1), 89–110.
Carter, C.H., Guy, D.E., 1988. Coastal erosion: processes, timing and magnitudes at the bluff toe. Mar. Geol. 84 (1–2), 1–17.
Carter, C.H., Monroe, C.B., Guy Jr., D.E., 1986. Lake Erie shore erosion: the effect of beach width and shore protection structures. J. Coast. Res. 2 (1), 17–23.
Chang, C., Xie, Z.Q., Xiong, G.M., Chu, L.M., 2011. The effect of flooding on soil physical and chemical properties of riparian zone in the Three Gorges Reservoir. J. Nat. Resour. 26 (7), 1236–1244 (in Chinese).
Cheng, R.M., Wang, X.R., Xiao, W.F., Guo, Q.S., 2010. Research progress of riparian zone. Sci. Silvae Sin. 46 (4), 111–119 (in Chinese).
Chinese academy of engineering, 2014. Stages Evaluation of Experimental Water Storage in Three Gorges Project. China Water & Power Press, Beijing (in Chinese).
Collins, B.D., Sitar, N., 2008. Processes of coastal bluff erosion in weakly lithified sands, Pacifica, California, USA. Geomorphology 97, 483–501.
Coops, H., Geilen, N., Verheij, H.J., Boeters, R., Van der Velde, G., 1996. Interactions between waves, bank erosion and emergent vegetation: an experimental study in a wave tank. Aquat. Bot. 53 (3–4), 187–198.
Couper, P., Stott, T., Maddock, A., 2002. Insights into river bank erosion processes derived from analysis of negative erosion-pin recordings: observations from three recent UK studies. Earth Surf. Process. Landf. 27, 59–79.
Cyberski, J., 1965. Denudation processes in the near-shore zone of the Roznów reservoir. Hydrolog. Serv. Bull. 1 (XIII), 63–64 (3,4).
Cyberski, J., 1973. Erosion of banks of storage reservoirs in Poland. Hydrol. Sci. J. 18 (3), 317–320.
Day, S.S., Gran, K.B., Belmont, P., Wawrzyniec, T., 2013. Measuring bluff erosion part 2: pairing aerial photographs and terrestrial laser scanning to create a watershed scale sediment budget. Earth Surf. Process. Landf. 38, 1068–1082.
de Moraes, M.V.A., Tommaselli, A.M.G., Santos, L.D., Rubio, M.F., Carvalho, G.J., Tommaselli, J.T.G., 2016. Monitoring bank erosion in hydroelectric reservoirs with mobile laser scanning. IEEE J. Sel. Top. Appl. Earth Obs. Remot. Sens. 9 (12), 5524–5532.
Dong, Y.P., Lu, H.S., Zhang, Q.G., Yan, L.J., 2009. Soil erosion of slopLand in the Yangtze Three Gorges Reservoir areas. J. Univ. JINAN 23 (1), 90–93 (in Chinese).
Du, Q., Zhong, Q.C., Wang, K.Y., 2010. Root effect of three vegetation types on shoreline stabilization of Chongming Island, Shanghai. Pedosphere 20 (6), 692–701.
Duru, U., 2017. Shoreline change assessment using multi-temporal satellite images: a case study of Lake Sapanca, NW Turkey. Environ. Monit. Assess. 189 (8), 385. http://dx.doi.org/10.1007/s10661-017-6112-2.
Fang, H.Y., Sun, L.Y., Tang, Z.H., 2014. Effects of rainfall and slope on runoff, soil erosion and rill development: an experimental study using two loess soils. Hydrol. Process. 29 (11), 2649–2658.
Fernandez, O.V.Q., Fulfaro, V.J., 2000. Rates and processes of bank erosion, Itaipu reservoir, Paraguay-Brazil border, South America. In: Cassia de Brito Galvao, T., Inyang, H. (Eds.), Proceeding of 5th International Symposium on Environmental Geotechnology and Global Sustainable Development, Minas Gerais, Brazil.
Gatto, L.W., Doe, W.W., 1987. Bank conditions and erosion along selected reservoirs. Environ. Geol. 9 (3), 143–154.
Ghimire, S.K., Higaki, D., Bhattarai, T.P., 2013. Estimation of soil erosion rates and eroded sediment in a degraded catchment of the Siwalik Hills, Nepal. Land 2 (3), 370–391.
Hagan, R.M., Roberts, E.B., 1972. Ecological impacts of water projects in California. J. Irrig. Drain. Div. 98, 25–48.
Hancock, G.R., Evans, K.G., 2010. Gully, channel and hillslope erosion—an assessment for a traditionally managed catchment. Earth Surf. Process. Landf. 35 (12), 1468–1479.
Hancock, G.R., Lowry, J.B.C., 2015. Hillslope erosion measurement—a simple approach to a complex process. Hydrol. Process. 29 (22), 4809–4816.
Harden, C.P., Foster, W., Morris, C., Chartrand, K.J., Henry, E., 2009. Rates and processes of streambank erosion in tributaries of the Little River, Tennessee. Phys. Geogr. 30 (1), 1–16.
Huang, Z.L., 2001. Biodiversity conservation for the three Gorges Project. Biodivers. Sci. 9 (4), 472–481 (in Chinese).
Hubertz, J.M., Driver, D.B., Reinhard, R.D., 1991. Wind waves on the Great Lakes: a 32 year hindcast. J. Coast. Res. 7 (4), 945–967.
Hudson, N.W., 1993. Field Measurement of Soil Erosion and Runoff. Food and Agriculture Organization of the United Nations, Rome.
Jiang, S.Q., Li, Q.Y., 1995. Relations between characteristics of purple soils and water and soil losses on upstream of Yangtze River. J. Yangtze River Sci. and Res. Inst. 12 (4), 51–57 (in Chinese).
Jin, C.X., 1996. The role of slope gradient on slope erosion. Geogr. Res. 15 (3), 57–63 (in Chinese).
Jing, K., Zhang, X.B., 2007. A discussion on natural sediment yield in the upper and middle Yangtze River. Geogr. Res. 26 (1), 67–74 (in Chinese).
Kaczmarek, H., Mazaeva, O.A., Kozyreva, E.A., Babicheva, V.A., Tyszkowski, S., Rybchenko, A.A., Brykala, D., Bartczak, A., Skowinski, M., 2016. Impact of large water level fluctuations on geomorphological processes and their interactions in the shore zone of a dam reservoir. J. Great Lakes Res. 42, 926–941.
Kao, L.S., Green, C.E., 2008. Analysis of variance: is there a difference in means and what does it mean? J. Surg. Res. 144 (1), 158–170.
Kearney, S.P., Fonte, S.J., García, E., Smukler, S.M., 2018. Improving the utility of erosion pins: absolute value of pin height change as an indicator of relative erosion. Catena 163, 427–432.

Kenwick, R.A., Shammin, M.R., Sullivan, W.C., 2009. Preference for riparian buffers. Landsc. Urban Plan. 91, 88–96.
Kim, H.Y., 2014. Analysis of variance (ANOVA) comparing means of more than two groups. Restor. Dent. Endod. 39 (1), 74–77.
Kociuba, W., Kubisz, W., Zagórski, P., 2014. Use of terrestrial laser scanning (TLS) for monitoring and modelling of geomorphic processes and phenomena at a small and medium spatial scale in polar environment (Scott River—Spitsbergen). Geomorphology 212, 84–96.
Kondratjev, N.E., 1966. Bank formation of newly established reservoirs. In: International Association Hydrological Sciences, Symposium Garda. 1. pp. 804–811.
Kronvang, B., Andersen, H.E., Larsen, S.E., Audet, J., 2013. Importance of bank erosion for sediment input, storage and export at the catchment scale. J. Soils Sediments 13, 230–241.
Lawler, D.M., 1991. A new technique for the automatic monitoring of erosion and deposition rates. Water Resour. Res. 27 (8), 2125–2128.
Lawler, D.M., 2008. Advances in the continuous monitoring of erosion and deposition dynamics: developments and applications of the new PEEP-3T system. Geomorphology 93 (1–2), 17–39.
Lawrence, P.L., 1994. Natural hazards of shoreline bluff erosion: a case study of Horizon view, lake Huron. Geomorphology 10 (1–4), 65–81.
Lawson, D.E., 1985. Erosion of Northern Reservoir Shores: An Analysis and Application of Pertinent Literature. US Army Corps of Engineers, Cold Regions Research & Engineering Laboratory.
Li, Q.Y., Jiang, S.Q., Sun, H.C., 1995. Determination of surface erosion of the small watersheds in the hilly area of purple soils in the upper reaches of the Yangtze River. J. Yangtze River Sci. and Res. Inst. 12 (1), 51–56 (in Chinese).
Li, K.F., Zhu, C., Wu, L., Huang, L.Y., 2013. Problems caused by the Three Gorges Dam construction in the Yangtze River basin: a review. Environ. Rev. 21 (3), 127–135.
Li, Y., Bao, Y.H., He, X.B., Wang, M.F., 2016. Spatial variability of nearshore wave height in typical reach of Three Gorges Reservoir: a case study from Zhong County. J. Chongqing Normal Univ. 33 (2), 43–48 (Nat. Sci.).
Lim, M., Petley, D.N., Rosser, N.J., Allison, R.J., Long, A.J., Pybus, D., 2005. Combined digital photogrammetry and time-of-flight laser scanning for monitoring cliff evolution. Photogramm. Rec. 20, 109–129.
Liu, B.Y., Nearing, M.A., Risse, L.M., 1994. Slope gradient effects on soil loss for steep slopes. T. ASAE 37 (6), 1835–1840.
Liu, Q.Q., Chen, L., Li, J.C., 2001. Influences of slope gradient on soil erosion. Appl. Math. Mech-En. 22 (5), 510–519.
Longoni, L., Papini, M., Brambilla, D., Barazzetti, L., Roncoroni, F., Scaioni, M., Ivanov, V.I., 2016. Monitoring riverbank erosion in mountain catchments using terrestrial laser scanning. Remote Sens. 8 (3), 241–263. http://dx.doi.org/10.3390/rs8030241.
Lorang, M.S., Stanford, J.A., 1993. Variability of shoreline erosion and accretion within a beach compartment of Flathead Lake, Montana. Limnol. Oceanogr. 38 (8), 1783–1795.
Lowrance, R.R., Airier, L.S., Williams, R.G., Inamdar, S.P., Sheridan, J.M., Bosch, D.D., Hubbard, R.K., Thomas, D.L., 2000. REMM: the riparian ecosystem management model. J. Soil Water Conserv. 55 (1), 27–34.
Lu, X.X., Higgitt, D.L., 2001. Sediment delivery to the three gorges: 2. Local response. Geomorphology 41 (2–3), 157–169.
Lukac, M., 1982. Failure of reservoir banks stability caused by wave abrasion. In: International Commission on Large Dams (Ed.), Proceeding of the 14th congress of international commission on Large Dams, Paris, France. III. pp. 1–10.
Mander, U., Kuusemets, V., Hayakawa, Y., 2005. Purification processes, ecological functions, planning and design of riparian buffer zones in agricultural watersheds. Ecol. Eng. 24, 421–432.
Nagle, G.N., Fahey, T.J., Woodbury, P.B., Ritchie, J.C., 2012. Bank erosion in fifteen tributaries in the Glaciated Upper Sesquehanna Basin of New York and Pennsylvania. Phys. Geogr. 33, 229–251.
Naiman, R.J., Decamps, H., 1997. The ecology of interfaces: riparian zones. Annu. Rev. Ecol. Syst. 28, 621–658.
Nasermoaddeli, M., Pasche, E., 2008. Application of terrestrial 3D laser scanner in quantification of the riverbank erosion and deposition. In: Altinakar, M. (Ed.), Proceedings of the International Conference on Fluvial Hydraulics (River flow 2008). Cesme-Ismir, Turkey, pp. 2407–2416.
New, T., Xie, Z.Q., 2008. Impacts of large dams on riparian vegetation: applying global experience to the case of China's Three Gorges Dam. Biodivers. Conserv. 17, 3149–3163.
Nilsson, C., Svedmark, M., 2002. Basic principles and ecological consequences of changing water regimes: riparian plant communities. Environ. Manag. 30 (4), 468–480.
Nilsson, C., Jansson, R., Zinko, U., 1997. Long-term responses of river-margin vegetation to water-level regulation. Science 276, 798–800.
Nunes, A.N., De Almeida, A.C., Coelho, C.O., 2011. Impacts of land use and cover type on runoff and soil erosion in a marginal area of Portugal. Appl. Geogr. 31 (2), 687–699.
Papanicolaou, A.N., Wilson, C.G., Tsakiris, A.G., Sutarto, T.E., Bertrand, F., Rinaldi, M., Dey, S., Langendoen, E., 2017. Understanding mass fluvial erosion along a bank profile: using PEEP technology for quantifying retreat lengths and identifying event timing. Earth Surf. Process. Landf. 42 (11), 1717–1732.
Pincus, H.J., 1962. Recession of Great Lakes shorelines. In: Pincus, H.J. (Ed.), Great Lake Basin. American Association for the Advancement of Science Publication 71, Baltimore, pp. 123–137.
Rando, C., Hopkinson, L., O'Neal, M., Fillhart, J., 2017. A method for assessing shoreline stability of alpine Lake, West Virginia. J. Contemp. Water Res. Educ. 160 (1), 85–99.
Reid, J.R., 1985. Bank-erosion processes in a cool-temperate environment, Orwell Lake, Minnesota. Geol. Soc. Am. Bull. 96, 781–792.
Reid, J.R., Sandberg, B.S., Millsop, M.D., 1988. Bank recession processes, rates and prediction, Lake Sakakawea, North Dakota, USA. Geomorphology 1, 161–189.
Rosser, N.J., Petley, D.N., Lim, M., Dunning, S., Allison, R.J., 2005. Terrestrial laser scanning for monitoring the process of hard rock coastal cliff erosion. Q. J. Eng. Geol. Hydrogeol. 38, 363–375.
Sadeghian, A., de Boer, D., Lindenschmidt, K.E., 2017. Sedimentation and erosion in Lake Diefenbaker, Canada: solutions for shoreline retreat monitoring. Environ. Monit. Assess. 189 (10), 507. http://dx.doi.org/10.1007/s10661-017-6217-7.
Saint-Laurent, D., Touileb, B.N., Saucet, J.P., Whalen, A., Gagnon, B., Nzakimuena, T., 2001. Effects of simulated water level management on shore erosion rates. Case study: Baskatong Reservoir, Québec, Canada. Can. J. Civ. Eng. 28 (3), 482–495.
Seversona, J.P., Nawrotb, J.R., Eichholzb, M.W., 2009. Shoreline stabilization using riprap breakwaters on a Midwestern reservoir. Lake Reservoir Manage. 25 (2), 208–216.
Shao, J.A., 2008. Characteristics of shape changes of river-way in the Chongqing reaches of the Yangtze River after impoundment of Three Gorges Reservoir. Res. Sci. 30 (9), 1431–1436 (in Chinese).
Shi, Z.L., Wen, A.B., Zhang, X.B., Yan, D.C., 2011. Comparison of the soil losses from 7Be measurements and the monitoring data by erosion pins and runoff plots in the Three Gorges Reservoir region, China. Appl. Radiat. Isot. 69 (10), 1343–1348.
Shur, I.L., Peretrukhin, N.P., Slavin-Borovskii, V.B., 1978. In: Grechishchev, S.E. (Ed.), Shore erosion in the cryolithosphere. Cryogenic Processes, Moscow: Nauta, pp. 57–73.
Simon, A., Collison, A.J.C., 2002. Quantifying the mechanical and hydrologic effects of riparian vegetation on streambank stability. Earth Surf. Process. Landf. 27 (5), 527–546.
Simon, A., Curini, A., Darby, S.E., Langendoen, E., 1999. Streambank mechanics and the role of bank and near-bank processes in incised channels. In: Darby, S.E., Simon, A. (Eds.), Incised Channels: Processes, Forms, Engineering and Managements. John Wiley & Sons, Chichester, pp. 123–152.
Siqueira, A.G., Azevedo, A.A., Dozzi, L.F.S., Duarte, H., 2015. Monitoring program of reservoir bank erosion at Porto Primavera Dam, Parana River, SP/MS, Brazil. Eng. Geol. Soc. Territory 3, 351–355.
Sirvent, J., Desir, G., Gutierrez, M., Sancho, C., Benito, G., 1997. Erosion ratesin badland areas recorded by collectors, erosion pins and profilometertechniques (Ebro basin, NE-Spain). Geomorphology 18, 61–75.
Stott, T.A., 2005. Natural recovery from accelerated forest ditch and stream bank erosion five years after harvesting of plantation forest on Plynlimon, mid-Wales. Earth Surf. Process. Landf. 30, 349–357.
Su, X.L., Nilsson, C., Pilotto, F., Liu, S.P., Shi, S.H., Zeng, B., 2017. Soil erosion and deposition in the new shorelines of the Three Gorges Reservoir. Sci. Total Environ. 599–600, 1485–1492.
Suleman, A.R., Pallu, M.S., Patanduk, J., Harianto, T., 2014. Experimental study of rainfall intensity effects on the slope erosion rate for silty sand soil with different slope gradient. Int. J. Eng. Tech. 4 (1), 58–63.
Tang, Q., Bao, Y.H., He, X.B., Zhou, H.D., Cao, Z.J., Gao, P., Zhong, R.H., Hu, Y.H., Zhang, X.B., 2014a. Sedimentation and associated trace metal enrichment in the riparian zone of the Three Gorges Reservoir, China. Sci. Total Environ. 479–480, 258–266.
Tang, Q., Bao, Y.H., He, X.B., Wen, A.B., 2014b. Heavy metal enrichment in the riparian sediments and soils of the Three Gorges Reservoir, China. IAHS Publ. 367, 244–251.
Thorne, C.R., 1981. Field measurements of rates of bank erosion and bank material strength. IAHS Publ. 133, 503–512.
Tommaselli, A.M., Moraes, M.V., Silva, L.S., Rubio, M.F., Carvalho, G.J., Tommaselli, J.T., 2014. Monitoring marginal erosion in hydroelectric reservoirs with terrestrial mobile laser scanner. In: Remondino, F., Menna, F. (Eds.), The International Archives of Photogrammetry, Remote Sensing and Spatial Information Sciences. XL-5. pp. 589–596.
Vandekerckhove, L., Poesen, J., Wijdenes, D.O., Gyssels, G., 2001. Short-term bank gully retreat rates in Mediterranean environments. Catena 44 (2), 133–161.
Vietz, G.J., Lintern, A., Webb, J.A., Straccione, D., 2017. River bank erosion and the influence of environmental flow management. Environ. Manag. 1–15. http://dx.doi.org/10.1007/s00267-017-0857-9.
Vilmundardóttir, O.K., Magnússon, B., Gísladóttir, G., Thorsteinsson, T., 2010. Shoreline erosion and Aeolian deposition along a recently formed hydro-electric reservoir, Blöndulón, Iceland. Geomorphology 114, 542–555.
Wang, J.C., Zhu, B., Wang, T., 2011. Characteristics of restoration of natural herbaceous vegetation of typical water-level fluctuation zone after flooding in the three gorges reservoir area. Resour. Environ. Yangtze Basin 20 (5), 603–610 (in Chinese).
Wang, Y.C., Lei, B., Zhang, S., 2012. Differences in vegetation and soil characteristics at different water-level altitudes in the drawdown areas of Three Gorges Reservoir area. J. Lake Sci. 24 (2), 206–212 (in Chinese).
Wolman, M.G., 1959. Factors influencing erosion of a cohesive river bank. Am. J. Sci. 257 (3), 204–216.
Wu, J.G., Huang, J.H., Han, X.G., Gao, X.M., He, F.L., Jiang, M.X., Jiang, Z.G., Primack, R.B., Shen, Z.H., 2004. The three gorges dam: an ecological perspective. Front. Ecol. Environ. 2 (5), 241–248.
Wynn, T.M., Mostaghimi, S., 2006. Effects of riparian vegetation on stream bank subaerial processes in southwestern Virginia, USA. Earth Surf. Process. Landf. 31 (4), 399–413.
Yang, F., Liu, W.W., Wang, J., Liao, L., Wang, Y., 2012. Riparian vegetation's responses to the new hydrological regimes from the Three Gorges Project: clues to revegetation in reservoir water-level-fluctuation zone. Acta Ecol. Sin. 32, 89–98.
Ye, C., Cheng, X.L., Zhang, Y.L., Wang, Z.X., Zhang, Q.F., 2012. Soil nitrogen dynamics following short-term revegetation in the water level fluctuation zone of the Three Gorges Reservoir, China. Ecol. Eng. 38 (1), 37–44.
Ye, C., Zhang, K.R., Deng, Q., Zhang, Q.F., 2013. Plant communities in relation to `flooding and soil characteristics in the water level fluctuation zone of the Three Gorges Reservoir, China. Environ. Sci. Pollut. Res. 20, 1794–1802.
Zaimes, G.N., Iakovoglou, V., Kosmadakis, I., Ioannou, K., Koutalakis, P., Ranis, G.,

Laopoulos, T., Tsardaklis, P., 2017. A new innovative tool to measure soil erosion. In: Water Resources in Arid Areas: The Way Forward. Springer, Cham, pp. 267–280.
Zhang, X.B., 2009. Thought on landform change of riparian zone of Three Gorges Reservoir. Bull. Soil Water Conserv. 29 (3), 1–5 (in Chinese).
Zhang, Q.F., Lou, Z.P., 2011. The environmental changes and mitigation actions in the Three Gorges Reservoir, China. Environ. Sci. Pol. 14 (8), 1132–1138.
Zhang, Z.Y., Wan, C.Y., Zheng, Z.W., Hu, L., Feng, K., Chang, J.B., Xie, P., 2013. Plant community characteristics and their responses to environmental factors in the water level fluctuation zone of the three gorges reservoir in China. Environ. Sci. Pollut. Res. 20, 7080–7091.
Zhu, B., Chen, S., You, X., Peng, K., Zhang, X.W., 2002. Soil fertility restoration on degraded upland of purple soil. Acta Pedol. Sin. 39 (5), 743–749 (in Chinese).
Zhu, N.N., Guo, Q.S., Qin, A.L., Pei, S.X., Ma, F.Q., Zhu, L., Jian, Z.J., 2015. Plant community dynamics in the Hydro-fluctuation Belt of the Three Gorges Reservoir at the Zigui and Wushan Section, East of Fengjie County, China. Acta Ecol. Sin. 35 (23), 7852–7867 (in Chinese).
Zuazo, V.H.D., Pleguezuelo, C.R.R., 2008. Soil-erosion and runoff prevention by plant covers. A review. Agron. Sustain. Dev. 28 (1), 65–86.